

# Internal Photoemission Spectroscopy for A PtSi/p-Si Schottky Junction

**B. ASLAN & R. TURAN**

*Physics Department, Middle East Technical University,  
06531 Ankara-TURKEY  
e-mail: aslan@metu.edu.tr*

Received 07.07.1999

## Abstract

Properties of internal photoemission in a PtSi-Si Schottky junction have been studied. The traditional Fowler plot of a detector's photoyield is found to be nonlinear for values close to the barrier height of the junction. It is shown that the model that takes all scattering mechanisms into account provides a successful description for the experimental results. It is also shown that the photoemission spectrum is independent of temperature in agreement with this model. The properties of detector's ambient influence the photoemission spectrum for wavelength of  $3 \mu\text{m}$  or less. A strong loss in the detector's response is observed at around  $3 \mu\text{m}$ . This drop is found to result from the ice formation on the detector's surface during the cooling process and it can be avoided by using a more effective pumping system.

## 1. Introduction

A PtSi-Si Schottky diode on p-type Si substrate can serve as an infrared detector in 3-5  $\mu\text{m}$  atmospheric window. In spite of its low quantum efficiency, it has been successfully integrated into commercial infrared imaging systems in recent years [1,2]. This success is obviously a result of the compatibility with the existing Si technology. It is thus important to know the response of PtSi-Si diodes to the infrared light. There have been many studies in this direction with investigations of the electrical [3] and optical [4,5,6,7,8,9] properties of PtSi-Si diodes on p-type substrates. The optical response of these diodes is usually analyzed by using the modified Fowler theory, but it does not represent a complete description of the photoemission process [10]. Several studies have been reported on a complete theoretical formulation of the internal photoemission in metal-semiconductor junctions, in particular PtSi-Si diodes [10,11,12,13]. Among them, Mooney and Silverman [10] developed a ballistic model that includes all possible scattering mechanisms in the

PtSi layer. However, the agreement between the experimental data and these theoretical models has not been well demonstrated.

Moreover, some other features of the internal photoemission in PtSi-Si diodes are still not well studied. For example, an anomaly (a dip) is sometimes observed in the photoemission spectrum of these diodes at around  $3 \mu\text{m}$  [14]. This dip was unreasonably attributed to parasitic barrier heights present at the junction. It is then of interest to investigate the reason of this anomaly which is also observed in this work.

The properties of internal photoemission in PtSi-Si are studied in this report. The experimental results are analyzed by using the most complete theoretical approach. It is shown that the model developed by Mooney and Silverman provides a successful description for the experimental results. The photoemission spectrum is found to be independent of temperature as predicted by this model. The effects of the vacuum conditions on the internal photoemission spectrum have also been studied. It is shown that the anomaly apparent around  $3 \mu\text{m}$  (0.4 eV) is related to the condensation of water vapor on the sample during the cooling process. The interpretation with a parasitic barrier is then shown to be incorrect.

## 2. Experimental details

### 2.1. Sample preparation

PtSi-Si diodes were fabricated on p-type (100) Si substrate with a resistivity of 25-30  $\Omega\cdot\text{cm}$ . The samples were first cleaned by using a standard RCA cleaning process. An oxide layer of  $1 \mu\text{m}$  was grown and patterned by the lithography for the guard ring production by ion implantation.  $^{31}\text{P}$  implantation with 35 keV at a dose of  $2.2 \times 10^{15} \text{ cm}^{-2}$  was carried out into regions of the diode's periphery for the n-type guard ring formation. The samples were then annealed at  $1000 \text{ }^\circ\text{C}$  for 30 min to activate the implanted ions. Following a new lithography to remove the oxide layer in the diode's active area, the samples were immediately loaded into a vacuum chamber. The photoresist used in this step was left on the sample's surface for the lift-off process used after the Pt evaporation. A Pt film of about  $50 \text{ \AA}$  thickness was evaporated on to the whole of the sample's surface by using the e-beam evaporation technique with an evaporation rate of  $1.5 \text{ \AA}/\text{sec}$ . The base pressure of the chamber before the evaporation was  $1 \times 10^{-6} \text{ Torr}$ , and it dropped to  $1 \times 10^{-5} \text{ Torr}$  during evaporation. Pt film in unwanted regions was removed by lifting the photoresist off from the surface. Ultrasonic agitation was necessary in several cases. Upon annealing at  $675 \text{ }^\circ\text{C}$  for 30 min under  $N_2$  atmosphere, Pt film that remained in the active region of the device was reacted with Si to form PtSi. The samples were finally fixed on a sample holder, which can be mounted into a closed cycle He cryostat. The electrical contacts to the samples were taken from the implanted guard ring and from the backside as shown in Fig. 1. The cryostat has a special window that permits infrared light to reach the sample surface.

## 2.2. Measurement Set-up

The experimental set-up for the internal photoemission measurements is shown in Fig. 2. A globar source is used for illuminating the sample. Before entering the monochromator, the light is filtered with a long pass filter with a cut-on wavelength of  $2.5 \mu\text{m}$ . By using a mirror system a small fraction of the monochromatic light at the exit of the monochromator is directed onto a CdHgTe detector after it is chopped at 70 Hz. The undeflected part of the light illuminates the photodiode mounted on the sample holder in the cryostat. The signals from the CdHgTe detector and from the PtSi-Si diode are measured by using a radiometer (RM) and an electrometer (EM), respectively. The measurements are controlled and recorded by a personal computer.

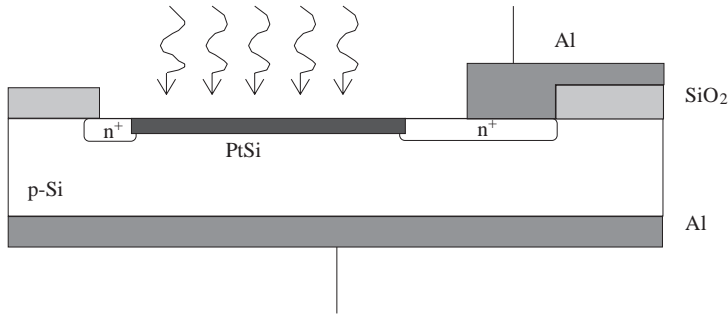


**Figure 1.** Cross-section of the PtSi-Si diode with guard ring.

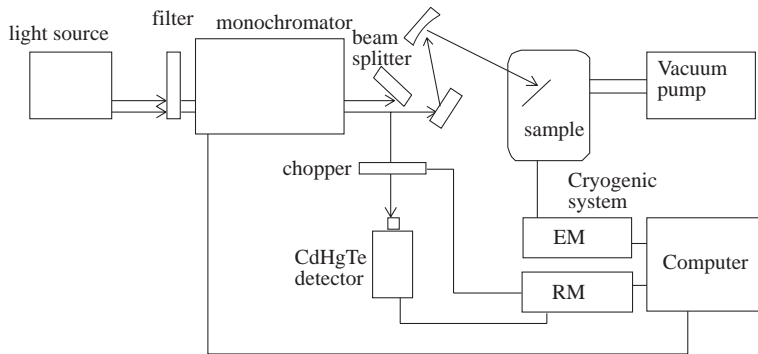


**Figure 2.** Optoelectronic spectral measurement system.

The yield of a photodiode is defined as the ratio of the number of photoelectrons to that of incident photons. The number of photoelectrons was determined directly from the measured photocurrent. The number of incident photons was estimated by measuring the light dropping on the sample by a calibrated CdHgTe detector. The amount of light absorbed or reflected light was determined by measuring the transmission spectrum

through the sample. The ratio between the reflected and absorbed data was estimated using previously reported results.

### 3. Features of PtSi-Si Response and Theoretical Consideration

Internal photoemission in a metal-semiconductor junction is traditionally described by the modified Fowler theory, according to which the following relation exists between photoyield and the incident wavelength [7,11]

$$Y_F = M^{1/2} \frac{(h\nu - \Phi)^2}{8E_F h\nu}, \quad (1)$$

where  $E_F$  is the Fermi energy,  $M$  is the ratio of the effective mass in the semiconductor to that in the metal film,  $h\nu$  is the incident photon energy and  $\Phi$  is the barrier height of the junction (can also be defined as threshold energy  $h\nu_0$  for photons). A plot of  $\sqrt{Y \cdot h\nu}$  vs  $h\nu$  should then yield a straight line whose intercept with the horizontal axis gives the barrier height. The Fermi energy can be determined from the slope of the same line.

The internal photoemission spectrum of a PtSi/p-Si diode is shown in Fig. 3. The dip seen at 0.4 eV results from water condensation on the sample and will be discussed later. When a straight line fitted to the linear part of the data, the barrier height and the Fermi level are found to be 0.273 eV and 1 eV, respectively. The value of the barrier height is higher than what is usually obtained from I-V measurements [5]. Also, the Fermi energy found from the slope is smaller than what is suggested for PtSi [16]. Another feature seen in Fig. 3 is that the experimental points do not follow the straight line of Eq. (1) especially for energies close to the barrier height. The effect of multiple reflections of the excited holes from the surfaces of the metal film and that of collisions with phonons, imperfections and cold electrons hold accountable for this discrepancy. These effects were first incorporated to the modified Fowler equation by Vickers [11] and Dalal [12]. In their models they made almost identical assumptions and used the same parameters for scattering variables. Then Mooney and Silverman improved this model for internal photoemission by removing some of these assumptions made in the Dalal's and Vickers' work.

According to this model, the internal yield  $Y$  in the photoemission process is given as [10]

$$Y = Y_0 + \left(1 - \frac{Y_0}{Y_\infty}\right) \gamma Y_1 + \left(1 - \frac{Y_0}{Y_\infty}\right) \left(1 - \frac{Y_1}{Y_\infty}\right) \gamma^2 Y_2 + \dots, \quad (2)$$

where  $\gamma$  is the probability that a hole will collide with a phonon before it collides with a cold electron,  $Y_\infty$  is the maximum quantum yield, and they are given as [10]

$$\gamma = \frac{L_e}{L_e + L_p} \text{ and } Y_\infty = \frac{h\nu - \Phi}{h\nu}. \quad (3)$$

For  $T = 0K$ ,  $M = 1$ ,  $E_F \gg h\nu > \Phi$  and neglecting the quantum mechanical effects [10]

$$Y_n = \frac{L^* U(d/L^*)}{8dE_F h\nu} (h\nu - n\hbar\omega - \Phi)^2 \quad (4)$$

Here  $d$  is the thickness of the PtSi film,  $\hbar\omega$  is the energy loss for each collision,  $n$  is the number of collisions and  $L^*$  is the attenuation length defined by

$$\frac{1}{L^*} = \frac{1}{L_e} + \frac{1}{L_p},$$

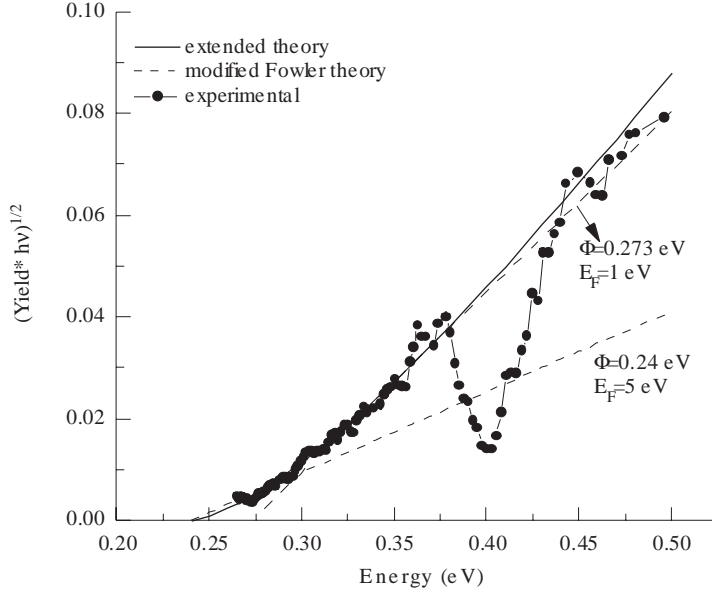


**Figure 3.** Internal photoemission spectrum of the PtSi-Si diode.

where  $L_e$  is the mean free path between collisions with cold electrons and  $L_p$  is the mean free path between semi-elastic collisions.  $U(d/L^*)$  is defined by an expression involving well-known exponential integrals which physically represent probabilities of having no bulk collisions during multiple traversals from the wall, averaged over distance and angular parameter: it is well approximated by  $[1 - \exp(-d/L^*)]$  [11]. Scattering by the film walls, by phonons and electrons and the energy lost during electron-phonon collisions are thus taken into account in the derivation of Eq. (2). In order to generate a computer fit to the experimental data Eq. (2) was used. The result is shown in Fig. 3.  $E_F$  was taken to be 5 eV which is within the suggested range for PtSi film.  $L_p$ ,  $L_e$ , and  $\hbar\omega$  were used as adjustable parameters in the fitting process. For the result displayed in Fig. 3,  $L_p = 60 \text{ \AA}$ ,  $L_e = 4000 \text{ \AA}$ ,  $\hbar\omega = 0.002 \text{ eV}$  [10]. These values are within the ranges suggested by Mooney and Silverman in their paper. The series in Eq. (2) is truncated at the integer  $n_{\max} = (h\nu - \Phi)/\hbar\omega$ , which corresponds to the thermalization of the hot hole. A perfect

fitting to the experimental data was obtained for the whole spectrum as shown in Fig. 3. The nonlinear part below 0.35 eV is well accounted for by this model. The barrier height used in this fitting is 0.24 eV which is consistent with the values measured usually by the I-V technique. For comparison the Fowler plot of Eq. (1) is plotted by using the barrier height and the Fermi energy values of the extended theory ( $\Phi = 0.24$  eV,  $E_F = 5$  eV) as shown in Fig. 3. It is seen that Eq. (1) predicts much lower yield than the extended theory for the same barrier height and Fermi energy values. One can then conclude that the extended theoretical approach that takes the scattering mechanisms into the account provides a more consistent explanation for the internal photoemission process.

#### 4. Temperature Dependence

The model including temperature dependence was first developed by Fowler and was later modified by Vickers. If the energy loss due to the collisions is adapted to the expression derived by Vickers for  $h\nu \geq \Phi$ , the yield as a function of temperature is found as

$$Y'_n(T) = \frac{L^*U(d/L^*)}{4dE_Fh\nu} \left[ \frac{(h\nu - n\hbar\omega - \Phi)^2}{2} + (kT)^2 \left\{ \frac{\pi^2}{6} + \sum_{i=1} \frac{1}{i^2} \left[ -\exp\left(-\frac{h\nu - n\hbar\omega - \Phi}{kT}\right) \right]^i \right\} \right] \quad (5)$$

This expression can be incorporated into the model described above by substituting it into Eq. (2) instead of Eq. (3). The spectrum of PtSi-Si diodes was calculated for different temperatures using Eq. (4) in Eq. (2). The results are displayed in Fig. 4a. It is seen that the internal photoemission is expected to be independent of temperature. This is verified by the experimental results shown in Fig. 4b. The experimental spectrum of the PtSi-Si samples obtained at 55 K, 70 K, 90 K are almost temperature independent. This result justifies the use of the theoretical description derived for  $T = 0$  K in the analysis for  $T > 0$ .

#### 5. Effect of Water Condensation on the Detector's Surface

In the photoemission spectrum shown in Fig. 3 and Fig. 4a dip is seen at about  $3 \mu\text{m}$ . The position of the dip along the horizontal axis is same in all measurements whereas its depth varies under different experimental conditions. This same dip was observed by others in similar experiments [14]. In order to see whether this dip is related to the detector's environment, the experiment was done using a mechanical pump and a diffusion pump. The starting pressure during the cooling down process was about  $1 \times 10^{-2}$  Torr,  $1 \times 10^{-4}$  Torr for the two cases, respectively. The photoemission spectrums under these conditions are shown in Fig. 5. It is seen that the dip disappeared when the detector's ambient is evacuated by a diffusion pump, which provides a better starting vacuum. In addition, when compared with the absorption spectrum of the ice, a correlation between

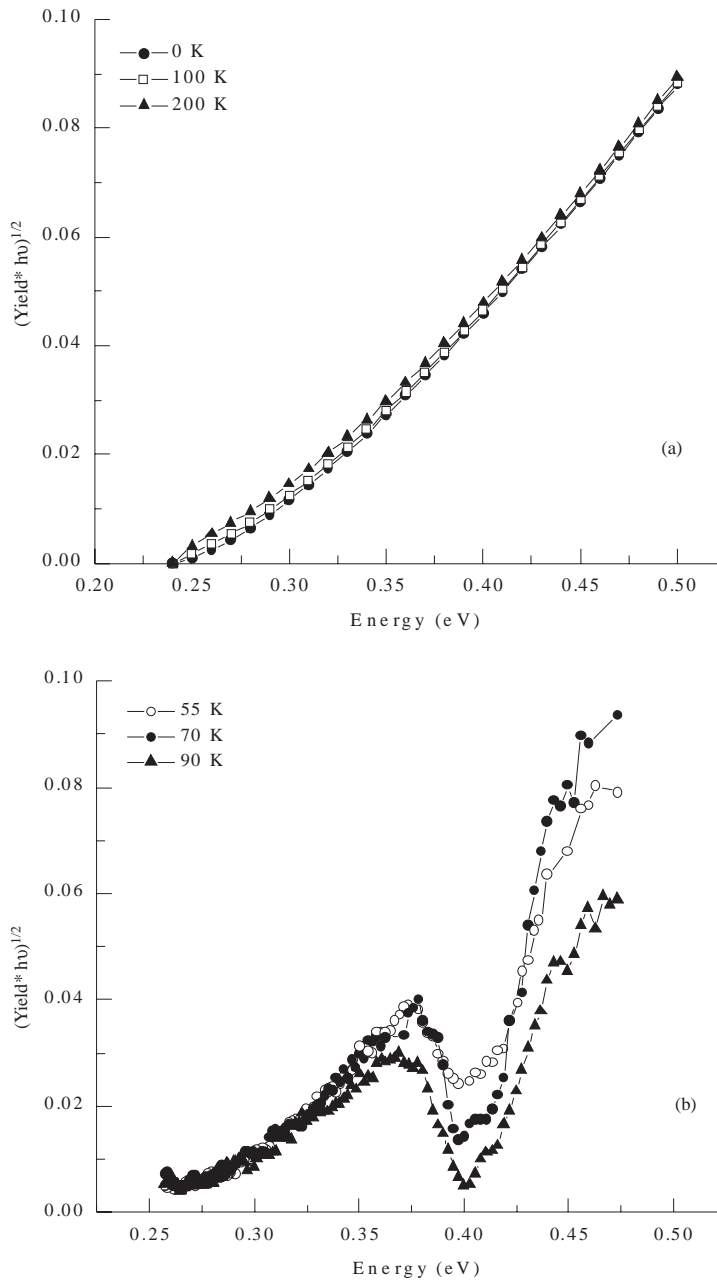


**Figure 4.** Temperature dependence of the internal photoemission obtained from (a) the extended model (b) the experimental measurements of the PtSi-Si diode.

the spectrums is clearly seen. The absorption spectrum of the ice [15], displayed in the inset of Fig. 5 has a strong absorption peak at  $3 \mu\text{m}$  and this coincides with the observed dip in our experiments. This indicates that the water vapor present in the ambient condenses on the detector's surface and forms a thin layer of ice upon cooling. This ice layer absorbs the incident light partly before it reaches the detector's surface. The water condensation is removed when the system is pumped out by a more effective pumping system. However, a new feature has emerged in the spectrum when the diffusion pump is used. The yield is seen to decrease above  $0.45 \text{ eV}$  as shown in Fig. 5. This new drop in the yield is likely to be related to the absorption by the oil vapor generated by the diffusion pump.

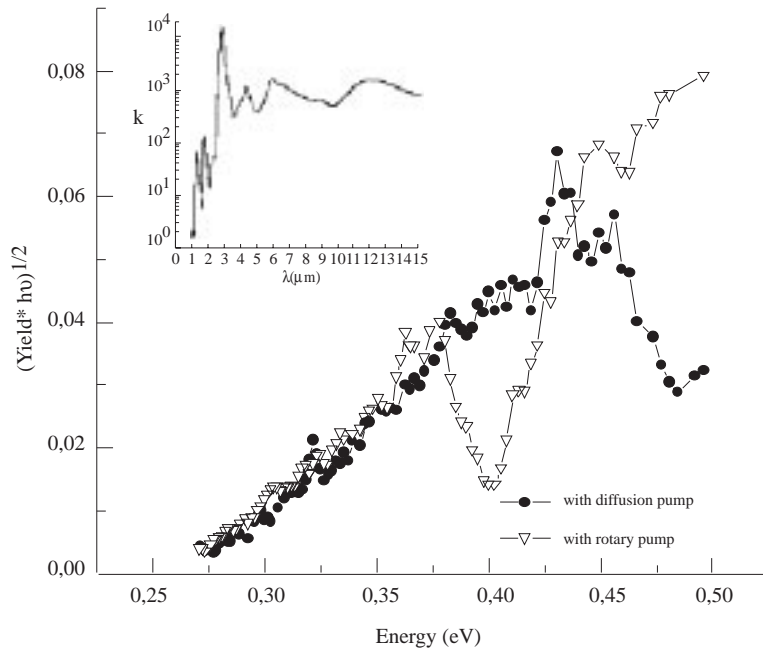


**Figure 5.** Internal Photoemission spectrum of the PtSi-Si diode for two different vacuum conditions.

In conclusion we have shown that the internal photoemission spectrum of a PtSi-Si diode can be described consistently by the theoretical model that includes the effects of scattering in the PtSi film. Temperature dependence of the model has been studied thereby it has been shown that the photoemission spectrum is little affected by the temperature variation. The experimental results agree well with this prediction. The effects of vacuum conditions on the internal photoemission spectrum have also been studied. It has been shown that the unexpected dip around  $0.4 \text{ eV}$  in spectrum is due to the absorption of light by the ice layer formed on sample's surface during the cooling process.



## References

- [1] W. F. Kosonocky, F. V. Shallcross, T. S. Villani, *IEEE Transactions on Electron Devices*, **ED-32**, 1564 (1985)
- [2] K. Konuma, S. T. Tohyama, A. Tanabe, N. Teranishi, K. Masubuchi, T. Saito, and T. Muramatsu, *IEEE Transactions on Electron Devices*, **39**, 1633 (1992)
- [3] V. W. L. Chin, J. W. V. Storey, and M. A. Green, *Solid-State Electronics*, **32**, 475 (1989)
- [4] H. Elabd and W. F. Kosonocky, *RCA Review*, **43**, 569 (1982)
- [5] V. W. L. Chin, J. W. V. Storey, and M. A. Green, *Solid-State Electronics*, **39**, 277 (1996)
- [6] J. M. Mooney, *J. Appl. Phys.* **65**, 2869 (1989)
- [7] J. Cohen, J. Vilms, R. J. Archer, Hewlett-Packard Labs, Palo Alto, CA, Final Rep., AFCRL-68-0651 (1968)
- [8] K. Komuma, Y. Asano, and K. Hirose, *Physical Review B*, **51**, 13 187 (1995)
- [9] A. Czernik, H. Palm, W. Cabanski, M. Schulz, and U. Suckow, *Appl. Phys. A* **55**, 180 (1992)
- [10] J. M. Mooney, J. Silverman, *IEEE Transactions on Electron Devices*, **ED-32**, 33 (1985)
- [11] V. E. Vickers, *Applied Optics*, **10**, 2190 (1971)
- [12] V. L. Dalal, *Journal of Applied Physics*, **42**, 2274 (1971)
- [13] D. E. Mercer and C. R. Helms, *J. Appl. Phys.* **65**, 5035 (1989)
- [14] X. Xiao, J. C. Sturm, S. R. Parihar, S. A. Lyon, D. Meyerhofer, S. Palfrey, and F. V. Shallcross, *IEEE Electron Device Letters*, **14**, 199 (1993)
- [15] W. M. Irvine and J. B. Pollack, *Icarus*, **8**, 324 (1958)
- [16] J. M. Mooney, PhD. University of Arizona (1986)